1-1-2015

Effects of core auditory cortex deactivation on neuronal response to simple and complex acoustic signals in the contralateral anterior auditory field

Andres Carrasco
Schulich School of Medicine & Dentistry

Melanie A. Kok
Schulich School of Medicine & Dentistry

Stephen G. Lomber
Schulich School of Medicine & Dentistry, steve.lomber@uwo.ca

Cerebral Cortex January 2015;25:84–96
doi:10.1093/cercor/bht205
Advance Access publication August 19, 2013

Effects of Core Auditory Cortex Deactivation on Neuronal Response to Simple and Complex Acoustic Signals in the Contralateral Anterior Auditory Field

Andres Carrasco[1,2], Melanie A. Kok[1,2] and Stephen G. Lomber[1,2]

[1]Brain and Mind Institute, Department of Physiology and Pharmacology, Schulich School of Medicine and Dentistry, University of Western Ontario, London, ON, Canada N6A 5C1 and [2]Cerebral Systems Laboratory, Department of Psychology, University of Western Ontario, London, ON, Canada N6A 5C2

Address correspondence to S.G. Lomber, Cerebral Systems Laboratory, Department of Physiology and Pharmacology, M216 Medical Sciences Building, University of Western Ontario, London, ON, Canada N6A 5C1. Email: steve.lomber@uwo.ca

Interhemispheric communication has been implicated in various functions of sensory signal processing and perception. Despite ample evidence demonstrating this phenomenon in the visual and somatosensory systems, to date, limited functional assessment of transcallosal transmission during periods of acoustic signal exposure has hindered our understanding of the role of interhemispheric connections between auditory cortical fields. Consequently, the present investigation examines the impact of core auditory cortical field deactivation on response properties of contralateral anterior auditory field (AAF) neurons in the *felis catus*. Single-unit responses to simple and complex acoustic signals were measured across AAF before, during, and after individual and combined cooling deactivation of contralateral primary auditory cortex (A1) and AAF neurons. Data analyses revealed that on average: 1) interhemispheric projections from core auditory areas to contralateral AAF neurons are predominantly excitatory, 2) changes in response strength vary based on acoustic features, 3) A1 and AAF projections can modulate AAF activity differently, 4) decreases in response strength are not specific to particular cortical laminae, and 5) contralateral inputs modulate AAF neuronal response thresholds. Collectively, these observations demonstrate that A1 and AAF neurons predominantly modulate AAF response properties via excitatory projections.

Keywords: cat, corpus callosum, interhemispheric, primary auditory cortex, reversible deactivation

Introduction

Neuroanatomical studies have revealed prominent networks of interhemispheric projections across sensory cortical areas [auditory (Diamond et al. 1968; Imig and Brugge 1978; Code and Winer 1985; Ruttgers et al. 1990; Rouiller et al. 1991; Morel et al. 1993; Liu and Suga 1997; Lee and Winer 2008a;); visual (Hubel and Wiesel 1967; Innocenti 1980; Cusick et al. 1984); somatosensory (Koralek and Killackey 1990; Carr and Sesack 1998)]. In visual and somatosensory cortices, this system of projections has been implicated in crucial functions of perception, including hemifield fusion (Choudhury et al. 1965; Hubel and Wiesel 1967; Payne 1990), midline receptive field (RF) extension (Antonini et al. 1979, 1983, 1985; Marzi et al. 1982), binocular activation (Berlucchi and Rizzolatti 1968; Lepore and Guillemot 1982; Blakemore et al. 1983; Payne et al. 1984), depth perception (Gardner and Cynader 1987), and RF organization (Pluto et al. 2005). In contrast to the well examined role of interhemispheric communication in visual and somatosensory modalities, the function of transcallosal projections in the auditory system remains poorly understood, and only recent investigations have demonstrated the crucial involvement of these connections to acoustic signal processing (Poremba et al. 2004; Tang et al. 2007; Carrasco and Lomber 2013).

Retrograde tracing investigations have provided evidence of a parallel network of interhemispheric projections between auditory fields (Lee et al. 2004). In the *felis catus,* this system of transcallosal pathways has been shown to amount to ~15% of all extrinsic connections to primary auditory cortex (A1) and anterior auditory field (AAF) neurons (Lee et al. 2004). While callosal projections to auditory fields arise principally (>50%) from homotopic contralateral fields, both A1 and AAF neurons supply strong and segregated heterotopic transcallosal connections to each other (5–50%) (Lee et al. 2004; Lee and Winer 2008a). Despite evidence demonstrating that projections emanating from A1 and AAF modulate contralateral A1 neuronal response activity via excitatory inputs, to date, functional properties of transcallosal projections to AAF have not been reported (Cipolloni and Peters 1983; Mitani and Shimokouchi 1985; Carrasco and Lomber 2013).

Models of acoustic processing have proposed that A1 and AAF participate in the earliest stages of cortical processing at a hierarchically equivalent level (Rouiller et al. 1991). While these models have been central to our understanding of cortical acoustic processing, expansion of this proposal necessitates information about functional contributions of interhemispheric projections. In an effort to bridge the gap between known connectional pathways of callosal projections and their functionality, the present study examined the effects of A1 and AAF neuronal silencing on contralateral AAF response activity levels. Based on known interhemispheric connectivity between AAF and core auditory areas (Diamond et al. 1968; Imig and Brugge 1978; Code and Winer 1985; Rouiller et al. 1991; Lee and Winer 2008a) and functional reports of transcallosal excitatory connections to primary auditory cortex (Cipolloni and Peters 1983; Mitani and Shimokouchi 1985; Carrasco and Lomber 2013), we hypothesized that deactivation of the principal sources of interhemispheric projections to AAF neurons should result in neuronal response strength declines during exposure to simple or complex acoustic signals. Data analyses confirmed our hypothesis and revealed that despite arrival of acoustic information to AAF via segregated parallel pathways from contralateral A1 and AAF neurons, on average, interhemispheric projections are excitatory and modulate AAF neuronal responses during acoustic exposure.

Materials and Methods

Overview

Neuronal responses to simple and complex acoustic signals were measured from the left hemisphere of 5 adult (>6 M) domestic cats

(*Felis catus*, Fig. 1*A*). Animals were housed in an enriched environment where social interactions and exposure to visual and acoustic signals were available daily via a television. Experimental procedures were performed in agreement with the National Research Council's *Guidelines for the Care and Use of Mammals in Neuroscience and Behavioral Research* (2003), the Canadian Council on Animal Care's *Guide to the Care and Use of Experimental Animals* (Olfert et al. 1993) and were approved by the University of Western Ontario Animal Use Subcommittee of the University Council on Animal Care. In-depth descriptions of methodological procedures have been reported (Carrasco and Lomber 2009a).

Cooling Loop and Head-Holder Implantation

Approximately 2 weeks prior to neuronal recording, animals underwent surgical cryoloop implantation procedures. Cryoloops of various shapes and sizes were assembled with 23-gauge stainless steel hypodermic tubing (Lomber 1999; Lomber et al. 1999). Twenty-four hours prior to surgical procedures animals were fasted and injected with dexamethasone (1.0 mg/kg, i.m.) was administered to reduce the incidence of edema. On the day of surgery, the cephalic vein was cannulated and an injection of sodium pentobarbital (~25 mg/kg i.v.) was administered to induce general anesthesia. Animals were then transferred to an aseptic surgical facility and attached to vital sign monitoring equipment. Animals were positioned in a stereotaxic frame (David Kopf Instruments, model 1530) and prepared for surgery (Carrasco and Lomber 2009a). Infusion of fluids (2.5% dextrose and half-strength lactated Ringer's solution) was initiated. A midline incision was made and the temporalis muscles were reflected laterally. Following craniotomy and durotomy of the right hemisphere, the cerebrum was exposed. Demarcation of auditory cortical fields was determined based on known anatomical markers (Reale and Imig 1980; Imaizumi et al. 2004; Carrasco and Lomber 2009a) and cryoloops of the appropriate size and shape were selected (Fig. 1*B*). A1 cooling loops (Lomber 1999; Lomber et al. 1999) were ~6-mm long and were positioned along the middle ectosylvian gyrus, amid the dorsal tips of the anterior and posterior ectosylvian sulci [about A4–A10 (stereotaxic coordinates are provided using the Horsley and Clarke (1908) system as described by Reinoso-Suárez (1961)); (Reale and Imig 1980); Fig. 1*B*]. Similar size cryoloops were placed over AAF (Knight 1977; Reale and Imig 1980; Phillips and Irvine 1982) on the crown of the anterior suprasylvian gyrus between A11 and A17 (Lomber and Malhotra 2008). Cortical cooling was tested by pumping chilled methanol through the lumen of the cryoloops. The extent of cortical surface cooling was measured with thermal imaging technology (FLIR, model SC325, Fig. 1*C*). Copper/constantan micro-thermistors attached to cryoloop unions measured loop temperature levels. Cooling loops were secured to the skull with dental acrylic. Subsequent to cooling loop placement, the exposed cerebrum was covered with the resected dura and Gelfilm®. The craniotomy was closed with dental acrylic.

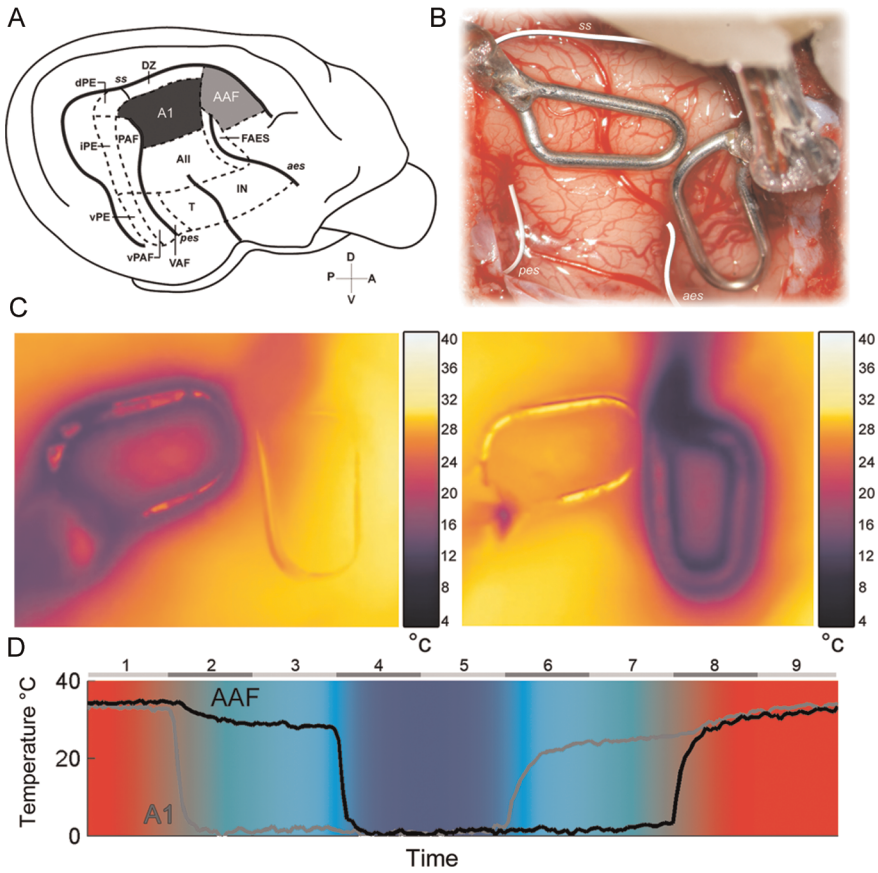

Figure 1. (*A*) Schematic illustration of cat cerebrum highlighting the 13 areas of auditory cortex in the left hemisphere. A1 is shown in black and AAF in gray. (*B*) Representative example of reversible cooling loop placement in an implanted animal. Thick white nonconnected lines show sulci location. (*C*) Representative example of cortical temperature changes during A1 (left panel) and AAF (right panel) cooling deactivation epochs. Cortical temperature changes and spread of cooling were measured during loop implantation with a thermal imaging camera. Colors represent temperature levels during a cooling epoch. Notice the restricted spread of cooling to adjacent cortical fields. (*D*) Changes in A1 and AAF cooling loop temperature during an entire recording cycle. Numbers on top represent the phase of the cycle, with even numbers indicating transitional temperature periods and odd numbers showing constant temperature epochs. Note that colors are presented as a guide of cortical temperature changes during cooling deactivation (blue cool, red warm) and are not associated with a color bar. A1, primary auditory cortex; AII, second auditory cortex; AAF, anterior auditory field; dPE, dorsal posterior ectosylvian area; DZ, dorsal zone of auditory cortex; FAES, auditory field of the anterior ectosylvian sulcus; IN, insular region; iPE, intermediate posterior ectosylvian area; PAF, posterior auditory field; T, temporal region; VAF, ventral auditory field; VPAF, ventral posterior auditory field; vPE, ventral posterior ectosylvian area. The sulci are indicated by italics: aes, anterior ectosylvian sulcus; ss, suprasylvian sulcus; pes, posterior ectosylvian sulcus. D, Dorsal; A, anterior; P, posterior; V, ventral.

Next, a head-holder was attached to the frontal bone. This process allowed positioning of the animal in the stereotaxic frame during electrophysiological recordings without the need of ear bars or pressure points, permitting unobstructed presentation of acoustic signals. The midline incision was closed with 3-0 silk sutures and Buprenorphine analgesic (0.01 mg/kg, i.m.) was administered during the first 3 days post awakening. In addition, systemic antibiotic and decreasing doses of dexamethasone were administered over a 1-week period. Postsurgical recovery processes were uneventful in all cases.

Surgical Preparation for Electrophysiological Recording

On the day of electrophysiological recordings, the cephalic vein was cannulated and a dose of sodium pentobarbital (25 mg/kg, i.v) was administered to induce anesthesia (Cheung et al. 2001). Incidence of edema and respiratory secretions was reduced by providing dexamethasone (1.0 mg/kg, i.v.) and atropine (0.03 mg/kg, s.c.) on a 12-h schedule. Hydration was accomplished with an infusion pump (2.5% dextrose/half-strength lactated Ringer's solution, 4 mL/kg/h, i.v.). Animals were intubated with an endotracheal tube. Electrocardiogram, blood oxygenation, and blood pressure measures were continuously monitored and supplemental doses of sodium pentobarbital were administered as needed to maintain a state of areflexia. Body temperature was maintained at 37°C with a water-filled heating pad (Gaymar, model T/pump). The animal was positioned in a stereotaxic frame (David Kopf Instruments, model 1530) using the previously implanted head holder (see Cooling loop and head-holder implantation section). A craniotomy was performed over AAF of the left hemisphere and the dura was resected. Desiccation was prevented by applying silicone oil to the exposed tissue. A picture of the exposed cerebrum was taken to document the location of microelectrode penetrations.

Stimulus Generation and Presentation

Neuronal recordings were conducted on a vibration-isolation table (Technical Manufacturing Corporation, model 63–500) within an electrically shielded double-walled sound chamber. The inside walls of the chamber were covered with 3″ thick acoustic isolation foam (Sonex, model SONEXone). A 24-bit D/A converter at 156 kHz (Tucker-Davis Technologies, model RX6) generated the acoustic signals and a transducer positioned 10 cm from the right ear delivered the signals in the free field (Tucker-Davis Technologies, model FF1). Simple and complex acoustic signals were calibrated with a ¼-inch microphone (Brüel and Kjær, model 4939). First, 3600 pure tones (25 ms long, 5 ms rise and fall times, cosine squared gated) varying in frequency (500–64 000 Hz in 1/32 octave steps) and amplitude (0–75 dB SPL in 5 dB steps) were presented in pseudorandom order per cooling phase. Second, animals were exposed to 600 white noise bursts per cooling cycle (25 ms long, 5 ms rise and fall times, cosine squared gated, bandwidth 1–32 kHz). Last, 1500 logarithmic frequency-modulated (FM) sweeps starting at 1, 2, 4, 8, 16, or 32 kHz and moving up or down from 1 to 5 octaves were presented at a rate of 2 Hz. Irrespective of frequency range or sweep direction, each FM group was presented 50 times (250 ms long) per cooling phase. The various starting and ending FM frequency points assured that a subset of signal ranges entered neuronal RFs in each recording cycle. Except for pure tones, acoustic signals were calibrated and delivered at 65 dB SPL. Acoustic signal features have been described in detail (Carrasco and Lomber 2011).

Reversible Cooling Deactivation

In the present investigation, we used tissue cooling deactivation methods to examine functional aspects of interhemispheric connectivity (Lomber 1999). This deactivation method was chosen for its numerous practical benefits. First, no local or distant tissue degeneration is induced during cooling epochs (Yang et al. 2006). Second, the primary effect of cooling is synaptic transmission disruption without affecting the activity of passing fibers (Jasper et al. 1970; Bénita and Condé 1972). Third, cooling deactivation permits regions of cerebral cortex to be deactivated and reactivated within minutes in a controlled and reproducible way (Lomber 1999). Last, cooling can be restricted to a small cortical region [for review see (Brooks 1983)].

The implanted cryoloops were connected to Teflon tubing submerged in a bath of dry ice and methanol, and A1 and/or AAF deactivation was induced by pumping chilled methanol through the tubing (Lomber et al. 1999). Cortical cooling levels were monitored from outside the acoustic chamber with a wireless thermometer (Omega, model UWTC-2). Temperatures were controlled within 1°C by varying the rate of methanol flow. Synaptic transmission is blocked at temperatures below 20°C (Bénita and Condé 1972; Adey 1974) via disruption of calcium channel activity. Thus, neuronal deactivation throughout the full thickness of cortex was achieved by lowering cooling loop temperatures to 3°, as this level lowers the base of layer VI to 20°C (Lomber et al. 1994, 1999, 2007; Lomber 1999; Lomber and Payne 2000; Palmer et al. 2007; Nakamoto et al. 2008; Antunes and Malmierca 2011; Anderson and Malmierca 2013;). The operational extent of deactivation was 2 mm orthogonal to the recording surface or an estimated volume of 70–75 mm^3.

Neuronal response activity to acoustic signals was recorded throughout 9 deactivation phases: 1) A1: warm, AAF: warm; 2) A1: cooling, AAF: warm; 3) A1: cool, AAF: warm; 4) A1: cool, AAF: cooling; 5) A1: cool, AAF: cool; 6) A1: rewarming, AAF: cool; 7) A1: rewarm, AAF: cool; 8) A1: rewarm, AAF: rewarming; 9) A1: rewarm, AAF: rewarm (Fig. 1*D*). Each phase lasted 5 min (noise exposure) or 30 min (FM sweep and pure tones), ensuring sufficient time for synaptic silencing and synaptic reactivation to transpire. Recording cycles began with a supplemental dose of sodium pentobarbital to assure that the highest levels of neuronal suppression produced by anesthesia were acquired during the first phase, and that subsequent variations in response activity could not be ascribed to anesthetic levels.

Recording Procedures

Extracellular neuronal responses across AAF laminae were measured with iridium axial array microelectrodes (FHC, model AM-003, 200 µm diameter). Cortical penetrations were limited to the anterior ectosylvian gyrus, lateral to the suprasylvian sulcus and anterior to the anterior ectosylvian sulcus. Electrode shafts contained 12 recording sites linearly spaced 150 µm apart with impedances between 1 and 3 MΩ (Fig. 2). Electrodes were positioned orthogonal to the cortical surface and advanced until the deepest (channel 1) and most superficial (channel 12) recording site revealed neuronal activity. This approach maximized the likelihood of acquiring neuronal responses from all layers of auditory cortex during individual cortical penetrations (Winer 1992). Despite the ability to record across cortical laminae, potential swelling and depression of cortical tissue during recording sessions in addition to vascular pulsations resulted in recording depth uncertainty. Therefore, recording channels were grouped as superficial (~150–600 µm, electrodes 9–12), middle (~750–1200 µm, electrodes 5–8), or deep (~1350–1800 µm, electrodes 1–4) cortical laminae (Fig. 2). Neuronal activity was band-pass filtered (500–5000 Hz), amplified (×10 000), and digitized at 25 000 Hz (Tucker-Davis Technologies, model RZ2).

Data Analysis

Offline single-unit sorting was conducted using Tucker-Davis Technologies software (OpenSort). Specifically, k-means clustering routines in combination with manual inspection of unit separation were used during sorting procedures. Only well-isolated units (maximum of 1 unit per recording site) within AAF boundaries were included for further analyses. While this procedure resulted in fewer units considered for in-depth scrutiny, it reduced the potential inclusion of simultaneously detected units by 2 or more recording sites. AAF location was determined based on tonotopy and response latency (Merzenich et al. 1973; Knight 1977; Reale and Imig 1980; Carrasco and Lomber 2011). A custom-made program (Matlab, Mathworks, Inc.) was used to construct 1-ms resolution peristimulus time histograms (PSTHs) for each of the 9 phases recorded within a cooling cycle (see Reversible cooling deactivation section). Response strength measures, defined as the maximum number of spikes per second (bin with highest response level regardless of time of occurrence), were calculated and compared

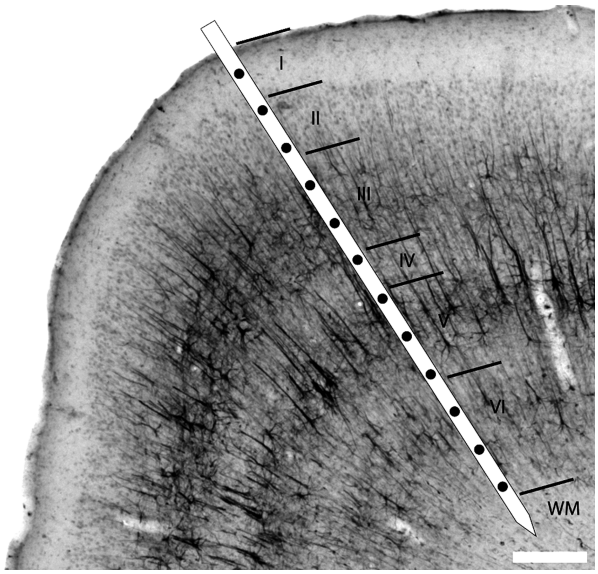

Figure 2. Photomicrograph of an SMI-32 stained coronal section showing AAF laminar organization with a schematic illustration of the recording electrode superimposed. The boundaries between cortical laminae are demarcated with black lines and labeled with roman numerals. The relative thickness of each layer is as follows (in μm): (I) 150, (II) 250, (III) 400, (IV) 150, (V) 400, and (VI) 450. Each of the 12 sites of the recording electrode is spaced 150 μm apart. Scale bar: 250 μm. Note that the photomicrograph shown was acquired from an animal not used in the present investigation and is used solely to illustrate AAF laminar thickness characteristics.

across cooling cycle phases. In an effort to reduce the possibility that variations in neuronal activity across cooling conditions were elicited by neuronal death, comparisons of response strength between cooling phases were limited to recordings where the first (A1: warm, AAF: warm) and last (A1: rewarm, AAF rewarm) phases of a recording cycle did not vary by more than ±20%. An experienced observer blind to stimulus conditions measured RF bandwidths and threshold levels. Bandwidths were defined as RF widths (expressed in octaves) in 5 dB SPL steps and neuronal thresholds as the minimum acoustic level (dB SPL) that reliably evoked neuronal activity (i.e., lower tip of RF). Lack of normality in response strength measures as determined by Kolmogorov–Smirnov tests impelled nonparametric statistical analyses. Statistical significance was assessed with Kruskal–Wallis tests ($P < 0.05$) followed by post hoc Tukey–Kramer corrections.

Results

Overview

Response activity of AAF neurons to simple and complex acoustic signals was measured before, during, and after epochs of contralateral A1 and/or AAF neuronal deactivation. Analyses of variations in neuronal discharge properties during deactivation epochs are presented in 3 parts. First, effects of contralateral cooling on AAF response strength are discussed. Second, variations in response magnitude as a function of AAF cortical laminae are examined. Last, the effects of contralateral neuronal silencing on RF properties are assessed.

Response Strength Properties

Noise Burst

Effects of A1 and/or AAF cooling deactivation on contralateral AAF neuronal activity were examined during periods of wideband noise exposure (n (single-units) = 158). Specifically,

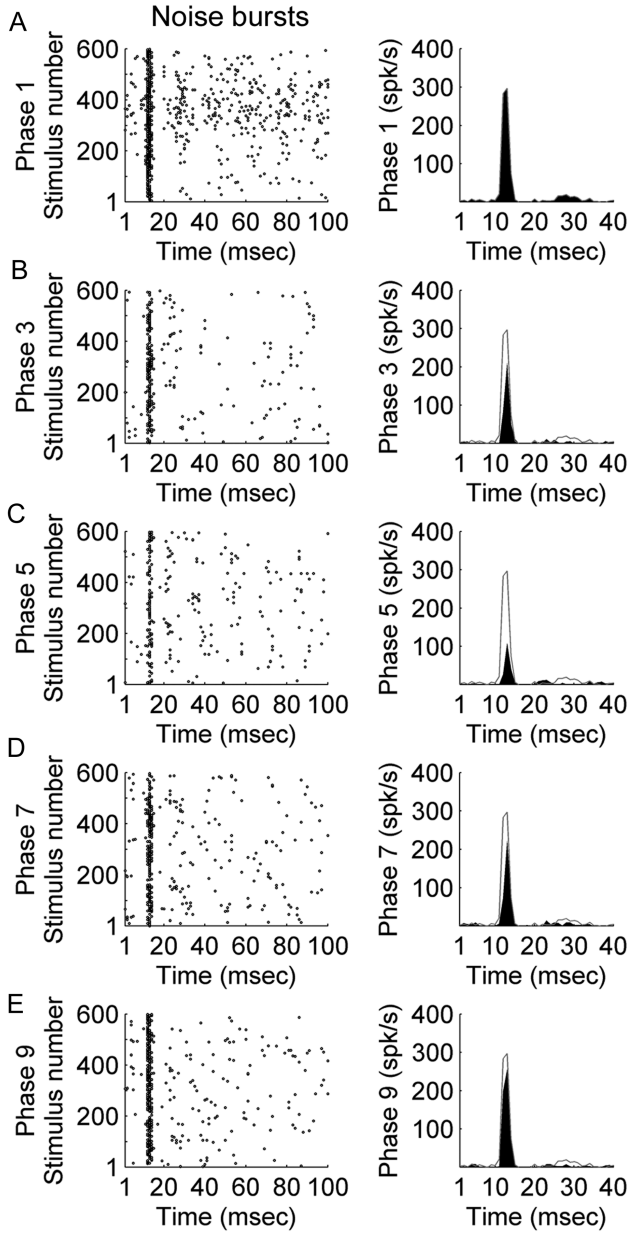

Figure 3. Representative example of AAF neuronal response strength properties during white noise burst exposure (3000 repetitions across 5 recording phases). PSTH and corresponding raster example of a single unit in AAF before contralateral cooling (phase 1, *A*), during contralateral A1 cooling (phase 3, *B*), during simultaneous contralateral A1 and AAF cooling (phase 5, *C*), during contralateral AAF cooling (phase 7, *D*), and after contralateral cooling (phase 9, *E*). Unfilled outlines in right column panels illustrate response level observed during warm condition.

neuronal peak response strength levels were measured and compared across cooling conditions. A representative case of changes in response strength magnitude observed is illustrated in Figure 3. Group data analyses revealed a significant ($P < 0.05$) decrease in AAF response strength of 22.73% during periods of contralateral A1 deactivation (Fig. 4*A*). The decrease in peak neuronal strength was further extended to 24.82% during the combined deactivation of contralateral A1 and AAF neurons ($P < 0.05$, Fig. 4*B*) and measured 11.34% during contralateral AAF deactivation alone (Fig. 4*C*). The revealed changes returned to baseline (warm condition) levels during

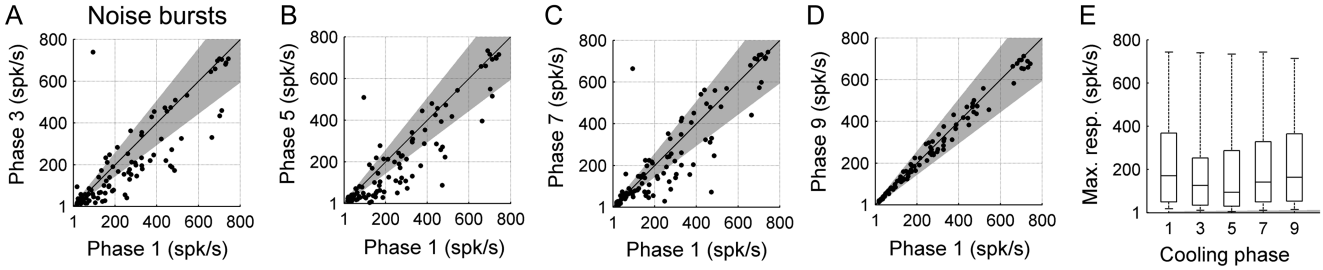

Figure 4. Comparison of AAF neuronal responses to noise burst exposure across cortical deactivation phases. (*A*) Peak response strength of AAF single units before (abscissa) and during (ordinate) contralateral A1 cooling (phase 3). (*B*) Peak response strength of AAF single units before (abscissa) and during (ordinate) simultaneous A1 and AAF contralateral deactivation (phase 5). (*C*) Peak response strength of AAF single units before (abscissa) and during (ordinate) contralateral AAF deactivation (phase 7). (*D*) Peak response strength of AAF single units before (abscissa) and after (ordinate) contralateral deactivation (phase 9). (*E*) Peak response strength group data. Boxplots illustrate lower quartile, median, and upper quartiles (horizontal box lines) and whiskers extend to most extreme values. Statistical significance decreases from baseline (phase 1) measures ($n = 158$ single units, Kruskal–Wallis tests, $P < 0.05$, followed by post hoc Tukey–Kramer corrections) were identified in phases 3 and 5. Shaded gray region demarcates ±25% of unity line (*A*–*D*). Cooling phases are explained in Figure 1*D*.

the rewarm condition (Fig. 4*D*). Collectively, these observations demonstrate that contralateral projections emanating in A1 and AAF and terminating in AAF neurons are predominantly excitatory and modulate AAF neuronal responses during wide-band noise exposure (Fig. 4*E*).

Frequency-Modulated Sweeps

In an effort to further explore the effects of contralateral deactivation on AAF activity during acoustic stimulation, AAF neuronal recordings were conducted during periods of upward and downward FM sweep exposure. In contrast to noise burst signals, FM sweeps varied in frequency range traveled. A representative example of the effects of A1 and/or AAF cooling deactivation on contralateral AAF activity is presented in Figure 5. Regardless of sweep direction (upward sweep: n (single units) = 153, downward sweep: $n = 164$), contralateral deactivation resulted in significant decreases in response strength in all conditions examined ($P < 0.05$). Specifically, deactivation of A1 neurons resulted in a 6.52% decrease in AAF response strength (8.42% upward sweep, 3.86% downward sweep, Fig. 6*A*). The observed decrease was further extended to 31.75% during the combined deactivation of A1 and AAF neurons (34.82% upward sweep, 27.44% downward sweep, Fig. 6*B*). Last, deactivation of AAF neurons alone elicited a decrease of 14.04% (13.48% upward sweep, 14.84% downward sweep, Fig. 6*C*) in AAF response strength. Comparisons between baseline (warm condition) and rewarm conditions revealed no significant changes in response strength (Fig. 6*D*). These results demonstrate that contralateral deactivation of primary and nonprimary auditory fields, results in decreases in peak response strength of AAF neurons during FM sweep exposure irrespective of sweep direction (Fig. 6*E*). Note that signal amplitude (65 dB SPL) and variations in sweep starting and ending frequencies points assured that a subset of signals entered neuronal RFs regardless of tuning characteristics.

Pure Tones

Effects of contralateral cooling on AAF response strength were measured during tonal exposure. A total of 32 400 pure tones were presented during each cooling cycle and changes in response strength between cooling phases were compared. A representative example of the effects of contralateral cooling on AAF activity is presented in Figure 7. Group data analyses revealed that in contrast to the variation in response properties observed during complex signal exposure (noise bursts and FM sweeps), AAF response strength did not significantly decline during contralateral A1 (3.78%) or A1/AAF (10.84%) cooling (n (single units) = 104, Figure 8*A*,B). However, AAF deactivation alone resulted in a significant decrease of 28.73% in contralateral AAF peak response strength ($P < 0.05$, Fig. 8*C*). AAF neuronal activity returned to baseline levels (warm phase) during the rewarm phase of the recording cycle (Fig. 8*D*,*E*).

Together, the changes in neuronal response properties observed across cooling conditions demonstrate 3 basic rules of interhemispheric communication between core auditory areas. First, on average, projections from A1 or AAF to contralateral AAF are primarily excitatory. This observation is supported by decreases in response strength across stimulus classes. Second, the magnitude of changes in response strength depends on acoustic features. While exposure to noise bursts and FM sweeps exhibited the largest decrease in response strength during the simultaneous deactivation of A1 and AAF neurons (29.03%), presentation of pure tones during the combined A1/AAF deactivation was only 10.84% and did not reach statistical significance. Third, cortical areas modulate AAF response properties based on acoustic properties. Exposure to noise bursts during AAF deactivation alone did not result in significant changes in response strength; in contrast, exposure to pure tones during the same cooling condition resulted in large decreases in response activity. In summary, while deactivation of contralateral core areas decreases AAF neuronal response strength, the presence and magnitude of these changes are modulated by acoustic features and field of deactivation.

Laminar Properties

Variations in response strength levels during contralateral deactivation epochs were analyzed as a function of cortical depth. Neuronal recordings were classified as deep (electrode 1 to electrode 4), mid (electrode 5 to electrode 8), or superficial (electrode 9 to electrode 12), and for each cortical depth group, changes in response strength were calculated.

Noise Bursts

Data analyses of deep ($n = 52$), mid ($n = 58$), and superficial layers ($n = 48$) during exposure to noise burst signals revealed decreases in response strength across AAF cortical depth. A median decrease of 28.89% in deep, 25.97% in mid, and 33.64% in superficial layers was measured during contralateral

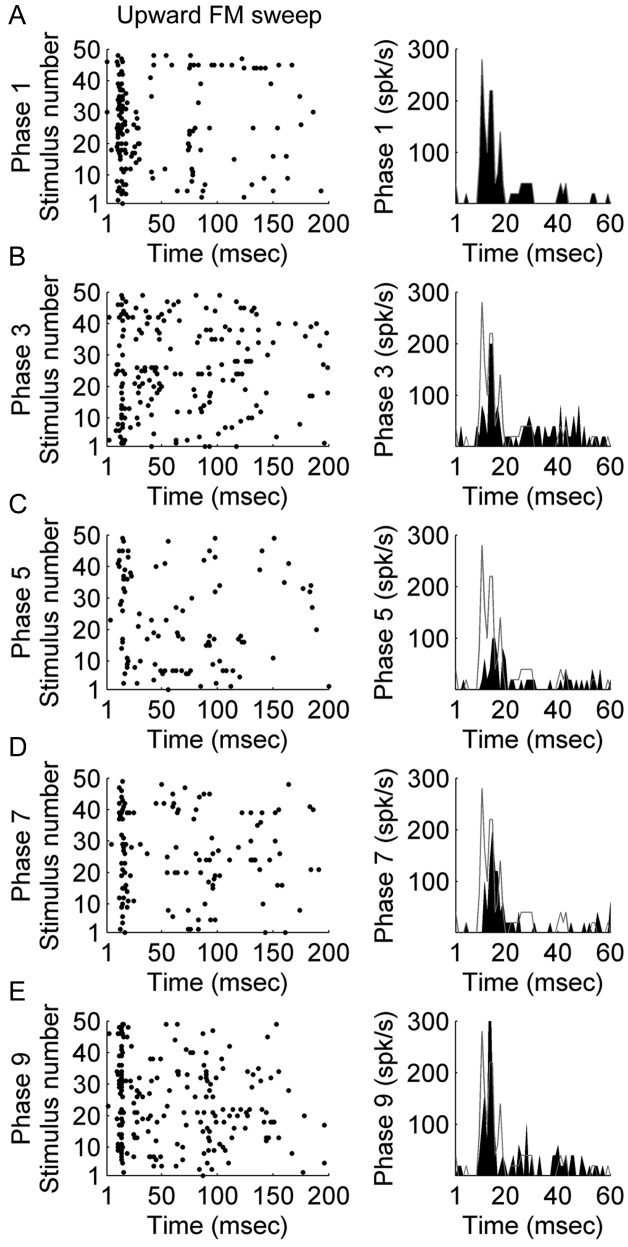

Figure 5. Representative example of AAF activity during exposure to 250 upward FM sweeps (116 kHz) across 5 recording phases. PSTH and corresponding raster example of a single unit recorded in A1 before contralateral cooling (phase 1, *A*), during contralateral A1 cooling (phase 3, *B*), during simultaneous contralateral A1 and AAF cooling (phase 5, *C*), during contralateral AAF cooling (phase 7, *D*), and after contralateral cooling (phase 9, *E*). Unfilled outlines in right column panels illustrate response level observed during warm condition.

A1 deactivation (Fig. 9*A*). During concurrent A1 and AAF deactivation median declines in peak activity measured 23.36% in deep, 37.57% in mid, and 38.39% in superficial layers (Fig. 9*A*). Last, AAF deactivation alone induced a median reduction of 13.81% in deep, 22.82% in mid, and 11.87% in superficial layers peak response strength (Fig. 9*A*). Statistical analyses did not reveal significant differences among laminar groups.

Frequency-Modulated Sweeps

Similar decreases in AAF response strength level during upward FM sweep and downward FM sweep exposure

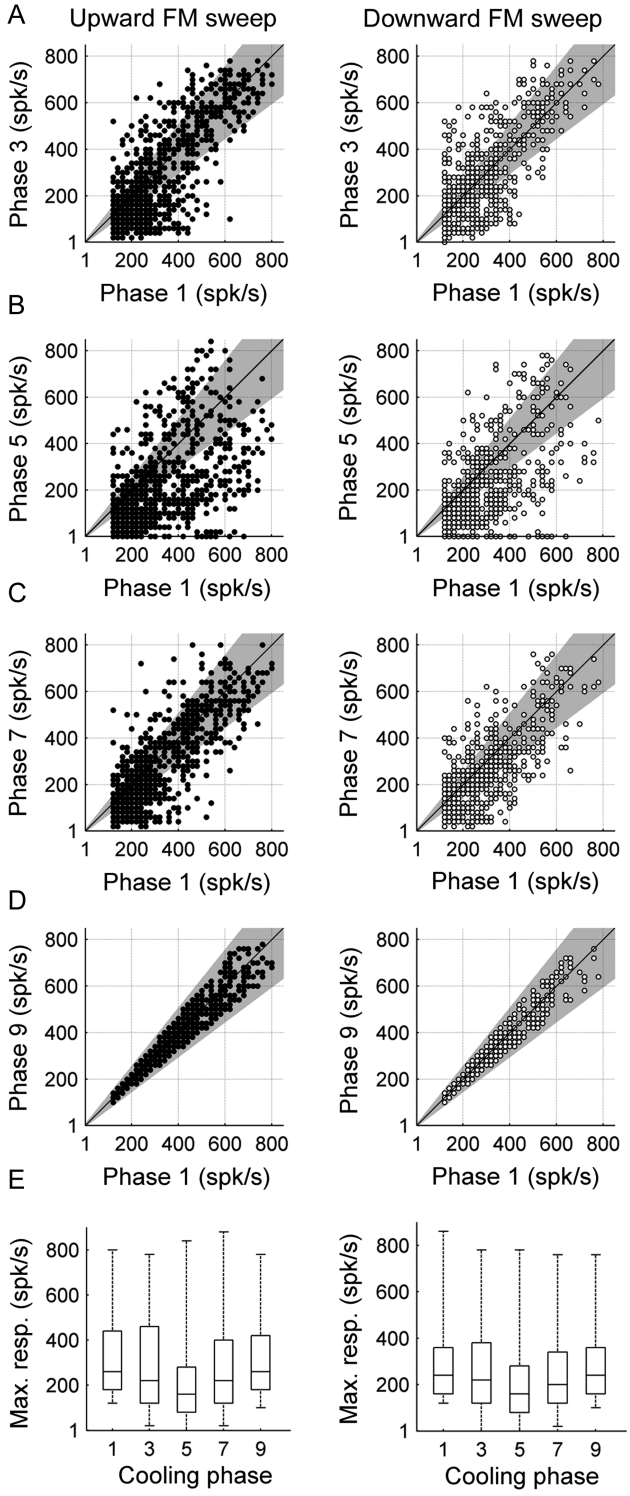

Figure 6. Comparison of AAF neuronal responses to upward (left column) and downward (right column) FM sweep exposure across cortical deactivation phases. (*A*) Peak response strength of AAF single units before (abscissa) and during (ordinate) contralateral A1 cooling (phase 3). (*B*) Peak response strength of AAF single units before (abscissa) and during (ordinate) simultaneous A1 and AAF contralateral deactivation (phase 5). (*C*) Peak response strength of AAF single units before (abscissa) and during (ordinate) contralateral AAF deactivation (phase 7). (*D*) Peak response strength of AAF single units before (abscissa) and after (ordinate) contralateral deactivation (phase 9). (*E*) Peak response strength group data. Boxplots illustrate lower quartile, median, and upper quartiles (horizontal box lines) and whiskers extend to most extreme values. Statistical significance decreases from baseline (phase 1) measures (upward FM sweeps, *n* (single units) = 153; downward FM

permitted the grouping and analysis of laminar response characteristics irrespective of sweep direction. In total, 90 deep, 123 mid, and 104 superficial single units were investigated. The median response strength of neurons decreased by 6.25% in deep, 9.45% in mid, and 13.51% in superficial layers during contralateral A1 deactivation epochs (Fig. 9*B*). The combined deactivation of A1 and AAF neurons resulted in a median decrease in response strength of 25.0% in deep, 37.50% in mid, and 50.0% in superficial layers (Fig. 9*B*). During periods of AAF deactivation alone, the median response strength levels of contralateral AAF neurons was reduced by 9.52% in deep, 20.0% in mid, and 25.0% in superficial layers (Fig. 9*B*). Statistical analyses (Kruskal–Wallis tests, $P < 0.05$, followed by post hoc Tukey–Kramer corrections) revealed that the observed changes in neuronal activity were significant between deep and superficial layers during A1 deactivation epochs, and across all laminar groups during AAF and A1/AAF deactivation periods.

Pure Tones

Changes in neuronal response properties to pure tones during deactivation of contralateral core auditory areas were examined in deep ($n = 34$), mid ($n = 35$), and superficial ($n = 35$) layers. Group data analyses revealed a median response strength decrease of 9.85% in deep, 0.0% in mid, and 7.50% in superficial layers during silencing of contralateral A1 neurons (Fig. 9*C*). Concurrent deactivation of A1 and AAF neurons resulted in a median response strength decrease of 14.19% in deep, 7.69% in mid, and 11.84% in superficial layers (Fig. 9*C*), and was extended to 26.14% in deep, 26.31% in mid, and 26.61% in superficial layers during AAF deactivation epochs alone (Fig. 9*C*). Statistical assessments (Kruskal–Wallis tests, $P < 0.05$, followed by post hoc Tukey–Kramer corrections) did not reveal differences in response change between laminar groups.

Receptive Field Properties

Relationships between response strength changes and RF structure were investigated by measuring variations in characteristic frequency (CF), neuronal threshold level, and RF bandwidth across contralateral cooling epochs of core auditory areas. CFs measured before, during and after cooling conditions did not significantly vary (Fig. 10*A*). In general, CFs were consistent across conditions, specifically, in over 94% (95.29% A1 cooling, 94.12% A1/AAF cooling, 95.30% AAF cooling) of neuronal recordings conducted CFs did not vary by more than 1 octave (Fig. 10*A*). In an attempt to avoid contamination of AAF recordings with A1 neuronal responses, microelectrode penetrations were kept away from the high frequency border shared by A1 and AAF neurons. While this approach minimized contamination of AAF recordings, it impeded the comparison of response changes between neurons tuned to low and high frequencies. Neuronal thresholds increased by 3.41, 6.11 ($P < 0.05$), and 6.06 ($P < 0.05$) dB SPL during deactivation epochs of A1, A1/AAF, and AAF, respectively (Fig. 10*B*). Last, group analyses of RF bandwidth measures did not reveal significant changes across cooling conditions (Fig. 10*C*). However, it is important to note that while on average analyses did not identify significant changes; variations in RF characteristics were observed in some recordings (Fig. 11). These results provide evidence that contralateral inputs from core auditory areas to AAF neurons can modulate threshold levels, but on average are not involved in CF or bandwidth regulation.

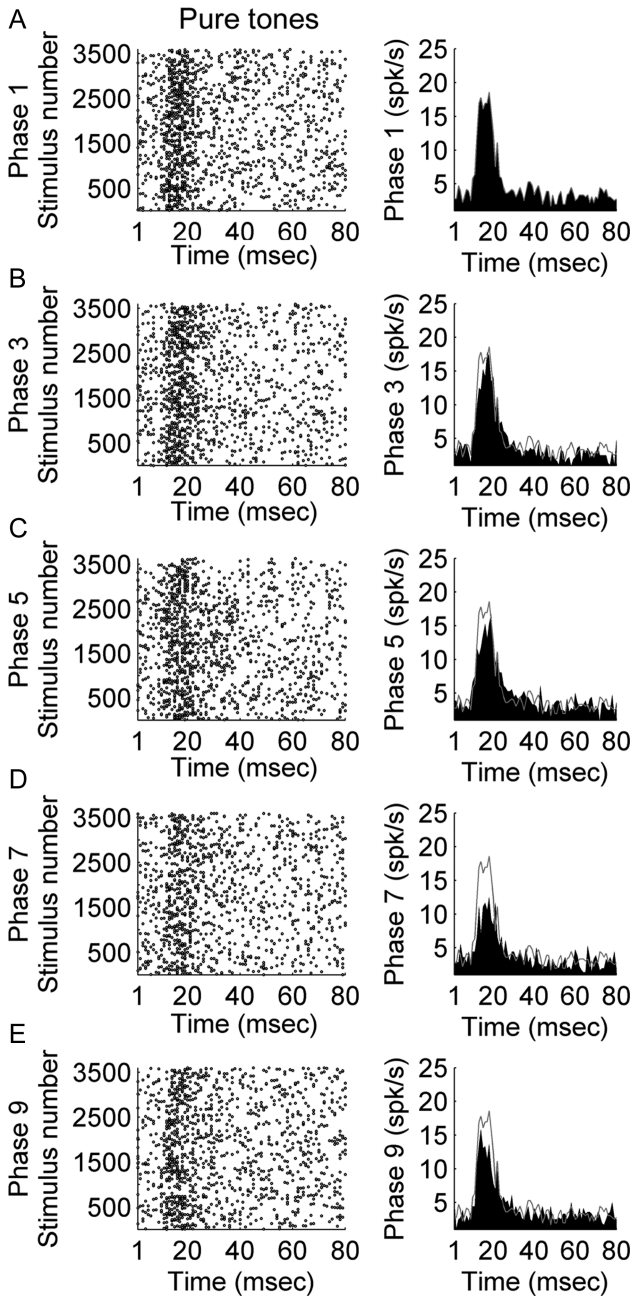

Figure 7. Representative example of AAF activity during exposure to 18 000 pure tones across 5 recording phases. PSTH and corresponding raster example of a single unit in A1 before contralateral cooling (phase 1, *A*), during contralateral A1 cooling (phase 3, *B*), during simultaneous contralateral A1 and AAF cooling (phase 5, *C*), during contralateral AAF cooling (phase 7, *D*), and during contralateral rewarm periods (phase 9, *E*). Unfilled outlines in right column panels illustrate response level observed during warm condition.

sweeps, *n* (single units) = 164, Kruskal–Wallis tests, $P < 0.05$, followed by post hoc Tukey–Kramer corrections) were identified in phases 3, 5, and 7 in both upward and downward sweep conditions. Shaded gray region demarcates ±25% of unity line (*A–D*). Cooling phases are explained in Figure 1*D*.

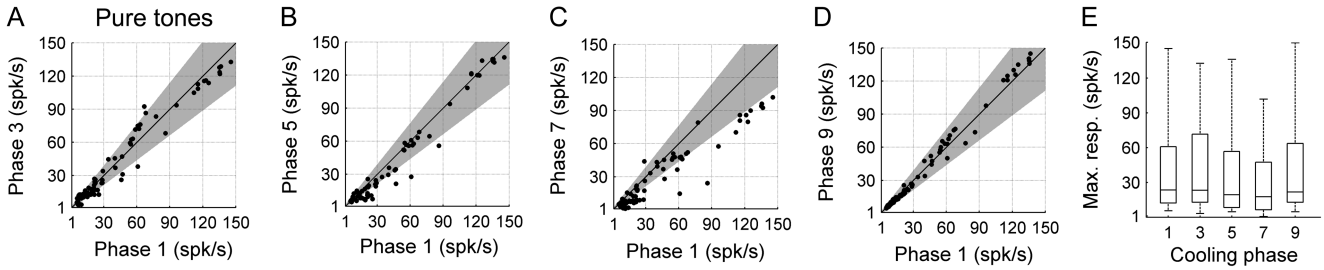

Figure 8. Comparison of AAF neuronal responses to pure tone exposure across cortical deactivation phases. (*A*) Peak response strength of A1 single units before (abscissa) and during (ordinate) contralateral A1 cooling (phase 3). (*B*) Peak response strength of A1 single units before (abscissa) and during (ordinate) simultaneous A1 and AAF contralateral deactivation (phase 5). (*C*) Peak response strength of A1 single units before (abscissa) and during (ordinate) contralateral AAF deactivation (phase 7). (*D*) Peak response strength of A1 single units before (abscissa) and after (ordinate) contralateral deactivation (phase 9). (*E*) Peak response strength group data. Boxplots illustrate lower quartile, median, and upper quartiles (horizontal box lines) and whiskers extend to most extreme values. Statistical significance decreases from baseline (phase 1) levels ($n = 104$ single units, Kruskal–Wallis tests, $P < 0.05$, followed by post hoc Tukey–Kramer corrections) were identified in phase 7. Shaded gray region demarcates ±25% of unity line (*A*–*D*). Cooling phases are explained in Figure 1D.

Discussion

Despite advances in our understanding of interhemispheric communication between cortical areas in visual (Innocenti 1980; Glickstein and Berlucchi 2008) and somatosensory (Clarey et al. 1996; Rema and Ebner 2003; Pluto et al. 2005) modalities, lack of comparable research in the auditory system has restricted the development of functional models of acoustic signal processing to ipsilateral networks of cortical connectivity. In an effort to expand this limited model of information processing, the present investigation examined the functional properties of core auditory cortical fields A1 and AAF on contralateral AAF response activity to acoustic exposure. Data analyses revealed that on average: 1) interhemispheric projections emanating from core auditory areas and terminating in contralateral AAF neurons are on average excitatory, 2) magnitude of changes in response strength vary based on acoustic features, 3) A1 and AAF projections can modulate AAF activity differently, 4) decreases in response strength are not specific to cortical depth, and 5) contralateral inputs can modulate AAF threshold levels but are not involved in CF or bandwidth modulation. Next, we discuss each of these findings in relation to known structural and functional properties of cortical networks.

A1 and AAF Projections to Contralateral AAF Are Predominantly Excitatory

The central result of the present investigation is the discovery that interhemispheric homotopic and heterotopic (A1) connections to AAF neurons are, on average, excitatory. This finding functionally characterizes known commissural connections in the *felis catus*, where it has been shown that the principal contralateral sources of projections to AAF emanate from AAF (>50%) and A1 (5–50%) neurons (Lee et al. 2004; Lee and Winer 2008a). These results are consistent with anatomical reports showing that commissural projections originate from glutamate expressing pyramidal neurons. Furthermore, the present investigation corroborates previous findings where deactivation of core cortical areas results in decreases of neuronal response levels in contralateral homotopic regions [auditory (Carrasco et al. 2013); visual (Payne et al. 1991); somatosensory (Rema and Ebner 2003)].

Changes in Response Strength Vary Based on Acoustic Features

Declines in response strength during contralateral deactivation epochs were associated with acoustic stimulus characteristics. Specifically, exposure to complex signals (noise bursts and FM sweeps) during A1 and A1/AAF deactivation epochs resulted in significant neuronal response strength reductions not present during pure tone presentation. This observation provides evidence that acoustic properties can impact the degree of neuronal response modulation. A plausible explanation for the observed phenomena is that distinct pathways of activation are engaged based on acoustic features. This proposition is supported by reports in the visual system where signal characteristics can result in different pathways of cortical activation (ffytche et al. 1995). However, much work will be needed to unravel the structural and functional principles of this observation.

Cortical Areas A1 and AAF Modulate Contralateral AAF Activity Differently

While exposure to pure tones during A1 deactivation did not result in contralateral AAF neuronal modulation, AAF cooling during the same acoustic condition resulted in significant declines in AAF peak response. This observation demonstrates that while both A1 and AAF have extensive projections to contralateral AAF neurons, transcallosal modulatory effects can be limited to a particular field during specific acoustic conditions (simple acoustic signals). This observation contrasts with the lack of modulatory properties observed during exposure to complex sounds and demonstrates that interhemispheric communication may be strongly modulated by acoustic signal properties as discussed above.

Decreases in Response Strength Are Present Across Cortical Laminae

In an effort to identify laminar differences in neuronal modulation, decreases in peak neuronal response strength were explored as a function of cortical depth. Laminar analyses revealed that irrespective of cortical depth, neuronal response strength was reduced during periods of contralateral deactivation. This observation is consistent with neuroanatomical studies that have demonstrated that callosal projections terminate across all cortical laminae (Kelly and Wong 1981; Code and Winer 1986; Aitkin et al. 1988). Additional support for decreases in response activity across layers has been shown in the visual (Payne et al. 1991) and somatosensory systems (Rema and Ebner 2003), where deactivation of V1 or S1 neurons result in response declines across all cortical layers in homotopic contralateral fields.

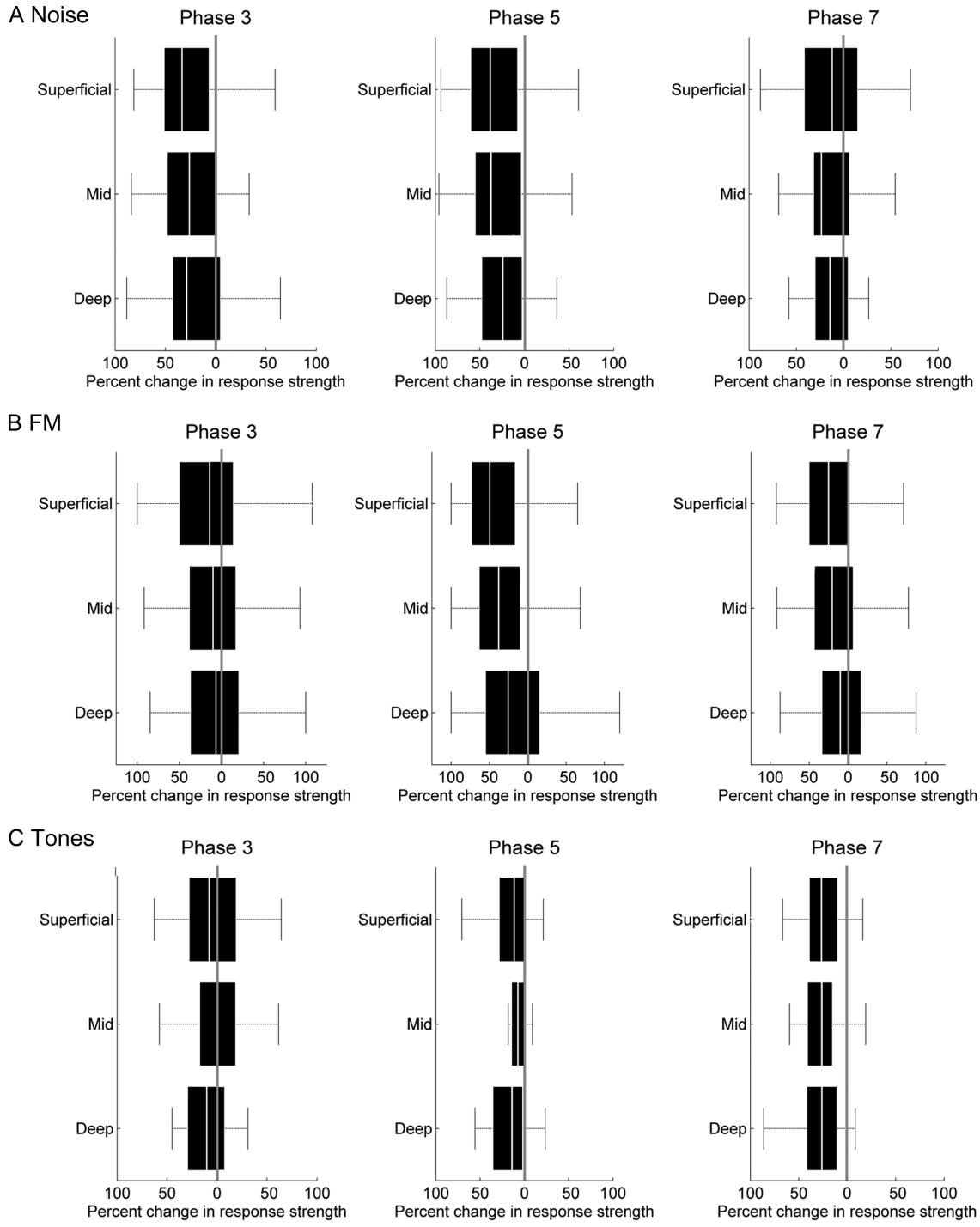

Figure 9. Comparison of neuronal peak response levels between warm (phase 1) and cooling epochs (A1: phase 3, A1/AAF: phase 5, AAF: phase 7) across laminar groups. (*A*) Peak neuronal response levels across cortical laminae during exposure to noise bursts (deep, $n = 52$; mid, $n = 58$; superficial, $n = 48$). (*B*) Peak neuronal response levels across cortical laminae during upward and downward FM sweep exposure (deep, $n = 90$; mid, $n = 123$; superficial, $n = 104$). (*C*) Peak neuronal response levels across cortical laminae during pure tone presentation (deep, $n = 34$; mid, $n = 35$; superficial, $n = 35$). Boxplots show lower quartile, median, and upper quartiles, and most extreme data values (whiskers). Statistically analyses (Kruskal–Wallis tests, $P < 0.05$, followed by post hoc Tukey–Kramer corrections) revealed significant changes in response level across laminar groups during FM sweep exposure in phases 3, 5, and 7 between deep-mid, deep-superficial, and mid-superficial neurons. In contrast, no significant changes in response magnitude across laminar groups were revealed during noise burst or pure tone exposure.

Contralateral Inputs Can Modulate AAF Threshold Levels But Are Not Involved in CF or Bandwidth Modulation

Analyses of RF changes during contralateral deactivation periods demonstrated that specific characteristics of AAF RFs can be modulated during contralateral A1/AAF silencing. In particular, group data analyses demonstrated a significant increase in neuronal threshold of 6.11 dB SPL during periods of combined A1 and AAF deactivation and of 6.06 dB SPL during AAF deactivation alone. The presence of threshold increases was contrasted by a lack of changes in RF widths or CF values.

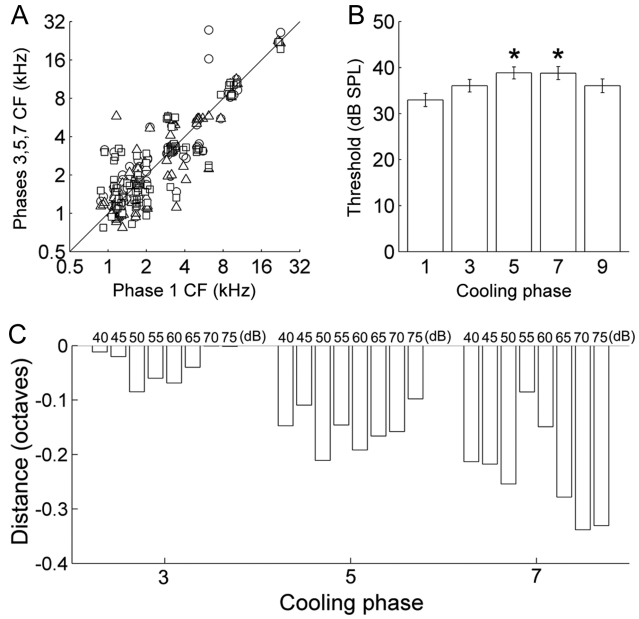

Figure 10. (*A*) Characteristic frequency (CF) values of AAF single units prior to cooling deactivation (phase 1), during contralateral A1 deactivation (phase 3), during simultaneous A1 and AAF deactivation (phase 5), and during AAF deactivation alone (phase 7). Symbols: circles, A1 deactivation; triangles, combined A1 and AAF deactivation; squares, AAF deactivation, $n = 104$. (*B*) Average neuronal response threshold levels of AAF single units before, during, and after contralateral cooling deactivation epochs. Statistical significance increases from baseline levels (phase 1) were identified in phases 5 and 7 ($n = 104$ single units, Kruskal–Wallis tests, $^*P < 0.05$, followed by post hoc Tukey–Kramer corrections). Error bars represent SE. (*C*) Changes in AAF receptive field bandwidth distance between precooling periods (phase 1) and during contralateral A1 deactivation (phase 3), combined A1 and AAF cooling periods (phase 5), and contralateral AAF silencing epochs (phase 7). Bandwidth measures are illustrated at 8 intensities above 0 dB SPL. Note that the marked decreases in bandwidth distance during cooling periods did not reach statistically significant levels, $n = 104$.

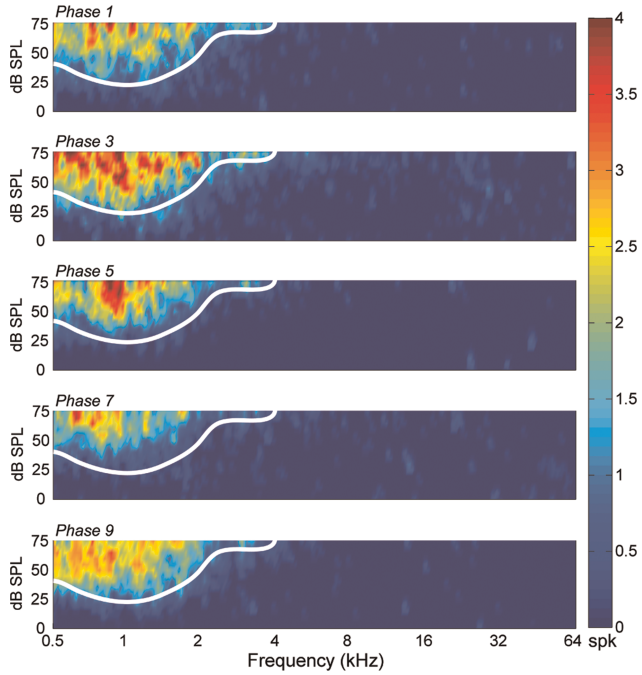

Figure 11. Representative effect of cooling deactivation on receptive field properties. Panels from top to bottom illustrate receptive field features of a single unit prior to cooling deactivation (phase 1), during contralateral A1 deactivation (phase 3), during simultaneous contralateral A1 and AAF deactivation (phase 5), during contralateral AAF deactivation alone (phase 7), and after cooling deactivation (phase 9, rewarm phase). Receptive field borders prior to cooling (white trace) are illustrated across all phases for comparative purposes. Note the decreases in bandwidth in phases 5 and 7.

These findings demonstrate that deactivation of core auditory fields can influence the sensitivity of neuronal thresholds without affecting the general shape of RFs. In contrast to ipsilateral connections among core auditory areas, where decreases in RF bandwidths have been observed, interhemispheric projections from core fields may not be involved in the modulation of RF shape or tuning (Carrasco and Lomber 2009a).

Comparisons to Previous Work

In a recent study by Carrasco and Lomber (2013) the effects of contralateral core auditory field deactivation on A1 response activity properties were examined. Comparisons of the present investigation with the findings of Carrasco and Lomber (2013) demonstrate copious similarities. First, both studies revealed that contralateral deactivation of core auditory fields result in a reduction of response activity levels across A1 (Carrasco and Lomber 2013) and AAF (present study). Second, decreases in neuronal response strength during periods of contralateral deactivation occur across all A1 and AAF cortical laminae. Third, despite increases in neuronal threshold levels, no significant changes in RF bandwidth were present during contralateral deactivation periods in either study. The similar findings between the 2 investigations demonstrate a common trend of modulatory properties by contralateral auditory fields on core auditory regions.

Interhemispheric Parallel and Segregated Pathways

Neuroanatomical tracing studies have demonstrated that interhemispheric projections from contralateral auditory cortical neurons to AAF cells account for approximately 15% of inputs to iso-frequency domains (Lee et al. 2004; Lee and Winer 2008a). Of this considerable contralateral input, 1% of AAF neurons express double-labeling when retrograde tracers are injected in contralateral A1 and AAF. These findings demonstrate that information flow to core auditory areas via callosal fibers is conducted primarily across parallel and independent pathways. The results of the present study provide information about how these connectional principles correlate to functional properties of acoustic information processing. First, distinctions in the effects of contralateral A1 or AAF deactivation on AAF activity demonstrate that parallel streams of information can modulate AAF neuronal responses differently. Second, significant changes in neuronal threshold levels during AAF but not during A1 deactivation demonstrate known distinctions in the magnitude of interhemispheric projections terminating in AAF neurons from contralateral AAF (>50%) and A1 (5–50%) cells. Third, regardless of the presence of segregated pathways of interhemispheric communication across auditory cortical fields, the present study establishes that both streams of information are predominantly excitatory.

Despite structural corroboration for many of the present findings, some of the results are intriguing and will require further structural and functional investigation. Specifically, during pure tone exposure, deactivation of AAF neurons resulted in larger decreases in contralateral AAF response strength (28.73%) than those observed during the concurrent deactivation of A1 and AAF neurons (10.84%). This finding

contradicts a predictable association between magnitude of excitatory input silencing and level of response strength decrease. While proposed structural models of acoustic information flow do not account for this functional observation, changes in cortico-thalamo-cortical interactions during deactivation periods may be involved in the observed phenomena. It remains for future investigations to reveal the functional principles of these connections and their effect on cortical activity.

Alternative Pathways

Despite strong structural evidence demonstrating a robust network of transcallosal projections in the auditory system (Diamond et al. 1968; Imig and Brugge 1978; Code and Winer 1985; Ruttgers et al. 1990; Rouiller et al. 1991; Morel et al. 1993; Liu and Suga 1997; Lee and Winer 2008a), alternative pathways of connectivity may explicate the observed phenomena. A plausible model of indirect interhemispheric communication capable of influencing AAF activity levels during contralateral A1/AAF deactivation, postulates that projections from core auditory areas to ipsilateral cochlear nuclei (CN) (Weedman and Ryugo 1996), followed by projections from CN neurons to contralateral superior olivary complex cells, propagate fluctuations in activity levels via feedforward projections that ultimately result in AAF neuronal response changes (Adams and Warr 1976; Hackney 1987; Thompson and Thompson 1991; Schofield and Cant 1996; Alibardi 2000; Arnott et al. 2004;). Despite evidence of changes in midbrain neuronal activity during epochs of cortical deactivation (Nakamoto et al. 2008) supporting this indirect pathway of modulation, the functionality of this system of projections remains poorly understood and much work will be needed to understand the role of this circuitry in interhemispheric neuronal modulation.

In addition to alternative pathways of communication between auditory cortical fields residing in opposite hemispheres, known connectivity between A1 and AAF neurons within a hemisphere present a challenge to the interpretation of the present dataset (Lee and Winer 2008b). Specifically, functional investigations into the role of connections between auditory cortical fields within the same hemisphere have demonstrated that deactivation of one auditory field often results in response strength declines in surrounding acoustically responsive cortical areas (Carrasco and Lomber 2009a, 2009b, 2010). Therefore, future investigations will be required to dissociate the individual modulatory influences of A1 or AAF deactivation on contralateral AAF activity.

Other Considerations

Anesthesia

An important consideration to the interpretation of the present results is the effect of anesthesia on cortical activity. In auditory cortex, it has been reported that administration of pentobarbital results in upregulation of GABAa receptors and increases in cellular membrane conductance (Zurita et al. 1994; Cheung et al. 2001; Gaese and Ostwald 2001). Therefore, administration of pentobarbital in the present investigation may have occluded inhibitory synaptic responses hindering the effects of callosal inputs on tuning bandwidth or callosal input-evoked inhibition. Hence, it is vital to acknowledge the inability to extend the present results to awake behaving states (Gaese and Ostwald 2003). Nonetheless, comparisons of the present results with previous reports suggest a plausible parallel between awake and anesthetized preparations. In particular, similar observations in response strength changes during contralateral deactivation have been observed in awake and anesthetized conditions [awake (Rema and Ebner 2003), halothane (Payne et al. 1991), ketamine (Clarey et al. 1996), and pentobarbital (present results)]. In addition, intracellular recordings have demonstrated neuronal response suppression during contralateral deactivation supporting the present results (Cipolloni and Peters 1983; Mitani and Shimokouchi 1985).

Loci of Deactivation

Despite the large region of cortical deactivation achieved in the present investigation, A1 neurons residing inside the posterior ectosylvian sulcus were considerably distant from optimal levels of cooling and may have not been deactivated. Thus, it is possible that the observed changes in response strength are an underestimation of the modulatory effects of contralateral A1 neurons on AAF activity.

Funding

This work was supported by grants from the Canadian Institutes of Health Research, the Natural Sciences and Engineering Research Council of Canada, and the Canada Foundation for Innovation.

Notes

We thank Pam Nixon and Amee J. Hall for technical and surgical assistance during this study. *Conflict of Interest:* None declared.

References

Adams JC, Warr WB. 1976. Origins of axons in the cat's acoustic striae determined by injection of horseradish peroxidase into severed tracts. J Comp Neurol. 170:107–121.

Adey WR. 1974. Biophysical and metabolic bases of cooling effects on cortical membrane potentials in the cat. Exp Neurol. 42:113–140.

Aitkin LM, Kudo M, Irvine DR. 1988. Connections of the primary auditory cortex in the common marmoset, callithrix jacchus jacchus. J Comp Neurol. 269:235–248.

Alibardi L. 2000. Cytology, synaptology and immunocytochemistry of commissural neurons and their putative axonal terminals in the dorsal cochlear nucleus of the rat. Ann Anat. 182:207–220.

Anderson LA, Malmierca MS. 2013. The effect of auditory cortex deactivation on stimulus-specific adaptation in the inferior colliculus of the rat. Eur J Neurosci. 37:52–62.

Antonini A, Berlucchi G, Lepore F. 1983. Physiological organization of callosal connections of a visual lateral suprasylvian cortical area in the cat. J Neurophysiol. 49:902–921.

Antonini A, Berlucchi G, Marzi CA, Sprague JM. 1979. Importance of corpus callosum for visual receptive fields of single neurons in cat superior colliculus. J Neurophysiol. 42:137–152.

Antonini A, Di Stefano M, Minciacchi D, Tassinari G. 1985. Interhemispheric influences on area 19 of the cat. Exp Brain Res. 59:171–184.

Antunes FM, Malmierca MS. 2011. Effect of auditory cortex deactivation on stimulus-specific adaptation in the medial geniculate body. J Neurosci. 23:17306–17316.

Arnott RH, Wallace MN, Shackleton TM, Palmer AR. 2004. Onset neurones in the anteroventral cochlear nucleus project to the dorsal cochlear nucleus. J Assoc Res Otolaryngol. 5:153–170.

Bénita M, Condé H. 1972. Effects of local cooling upon conduction and synaptic transmission. Brain Res. 36:133–151.

Berlucchi G, Rizzolatti G. 1968. Binocularly driven neurons in visual cortex of split-chiasm cats. Science. 159:308–310.

Blakemore C, Diao YC, Pu ML, Wang YK, Xiao YM. 1983. Possible functions of the interhemispheric connexions between visual cortical areas in the cat. J Physiol. 337:331–349.
Brooks V. 1983. Study of brain function by local, reversible cooling. Rev Physiol Biochem Pharmacol. 95:1–109.
Carr DB, Sesack SR. 1998. Callosal terminals in the rat prefrontal cortex: synaptic targets and association with GABA-immunoreactive structures. Synapse. 29:193–205.
Carrasco A, Brown TA, Kok M, Chabot N, Kral A, Lomber SG. 2013. Influence of core auditory cortical fields on acoustically-evoked activity in contralateral primary auditory cortex. J Neurosci. 33:776–789.
Carrasco A, Lomber SG. 2009a. Differential modulatory influences between primary auditory cortex and the anterior auditory field. J Neurosci. 29:8350–8362.
Carrasco A, Lomber SG. 2009b. Evidence for hierarchical processing in cat auditory cortex: nonreciprocal influence of primary auditory cortex on the posterior auditory field. J Neurosci. 29: 14323–14333.
Carrasco A, Lomber SG. 2013. Influence of core auditory cortical areas on acoustically evoked activity in contralateral primary auditory cortex. J Neurosci. 33:776–789.
Carrasco A, Lomber SG. 2011. Neuronal activation times to simple, complex, and natural sounds in cat primary and nonprimary auditory cortex. J Neurophysiol. 106:1166–1178.
Carrasco A, Lomber SG. 2010. Reciprocal modulatory influences between tonotopic and nontonotopic cortical fields in the cat. J Neurosci. 30:1476–1487.
Cheung SW, Nagarajan SS, Bedenbaugh PH, Schreiner CE, Wang X, Wong A. 2001. Auditory cortical neuron response differences under isoflurane versus pentobarbital anesthesia. Hear Res. 156:115–127.
Choudhury BP, Whitteridge D, Wilson ME. 1965. The function of the callosal connections of the visual cortex. Q J Exp Physiol Cogn Med Sci. 50:214–219.
Cipolloni PB, Peters A. 1983. The termination of callosal fibres in the auditory cortex of the rat. A combined golgi—electron microscope and degeneration study. J Neurocytol. 12:713–726.
Clarey JC, Tweedale R, Calford MB. 1996. Interhemispheric modulation of somatosensory receptive fields: evidence for plasticity in primary somatosensory cortex. Cereb Cortex. 6:196–206.
Code RA, Winer JA. 1986. Columnar organization and reciprocity of commissural connections in cat primary auditory cortex (AI). Hear Res. 23:205–222.
Code RA, Winer JA. 1985. Commissural neurons in layer III of cat primary auditory cortex (AI): pyramidal and non-pyramidal cell input. J Comp Neurol. 242:485–510.
Cusick CG, Gould HJ 3rd, Kaas JH. 1984. Interhemispheric connections of visual cortex of owl monkeys (Aotus trivirgatus), marmosets (Callithrix jacchus), and galagos (Galago crassicaudatus). J Comp Neurol. 230:311–336.
Diamond IT, Jones EG, Powell TP. 1968. Interhemispheric fiber connections of the auditory cortex of the cat. Brain Res. 11:177–193.
ffytche DH, Guy CN, Zeki S. 1995. The parallel visual motion inputs into areas V1 and V5 of human cerebral cortex. Brain. 118(Pt 6):1375–1394.
Gaese BH, Ostwald J. 2001. Anesthesia changes frequency tuning of neurons in the rat primary auditory cortex. J Neurophysiol. 86:1062–1066.
Gaese BH, Ostwald J. 2003. Complexity and temporal dynamics of frequency coding in the awake rat auditory cortex. Eur J Neurosci. 18:2638–2652.
Gardner JC, Cynader MS. 1987. Mechanisms for binocular depth sensitivity along the vertical meridian of the visual field. Brain Res. 413:60–74.
Glickstein M, Berlucchi G. 2008. Classical disconnection studies of the corpus callosum. Cortex. 44:914–927.
Hackney CM. 1987. Anatomical features of the auditory pathway from cochlea to cortex. Br Med Bull. 43:780–801.
Horsley V, Clarke RH. 1908. The structure and function of the cerebellum examined by a new method. Brain. 31:45–124.
Hubel DH, Wiesel TN. 1967. Cortical and callosal connections concerned with the vertical meridian of visual fields in the cat. J Neurophysiol. 30:1561–1573.
Imaizumi K, Priebe NJ, Crum PA, Bedenbaugh PH, Cheung SW, Schreiner CE. 2004. Modular functional organization of cat anterior auditory field. J Neurophysiol. 92:444–457.
Imig TJ, Brugge JF. 1978. Sources and terminations of callosal axons related to binaural and frequency maps in primary auditory cortex of the cat. J Comp Neurol. 182:637–660.
Innocenti GM. 1980. The primary visual pathway through the corpus callosum: morphological and functional aspects in the cat. Arch Ital Biol. 118:124–188.
Jasper HH, Shacter DG, Montplaisir J. 1970. The effect of local cooling upon spontaneous and evoked electrical activity of cerebral cortex. Can J Physiol Pharmacol. 48:640–652.
Kelly JP, Wong D. 1981. Laminar connections of the cat's auditory cortex. Brain Res. 212:1–15.
Knight PL. 1977. Representation of the cochlea within the anterior auditory field (AAF) of the cat. Brain Res. 130:447–467.
Koralek KA, Killackey HP. 1990. Callosal projections in rat somatosensory cortex are altered by early removal of afferent input. Proc Natl Acad Sci USA. 87:1396–1400.
Lee CC, Imaizumi K, Schreiner CE, Winer JA. 2004. Concurrent tonotopic processing streams in auditory cortex. Cereb Cortex. 14:441–451.
Lee CC, Winer JA. 2008a. Connections of cat auditory cortex: II. commissural system. J Comp Neurol. 507:1901–1919.
Lee CC, Winer JA. 2008b. Connections of cat auditory cortex: III. corticocortical system. J Comp Neurol. 507:1920–1943.
Lepore F, Guillemot JP. 1982. Visual receptive field properties of cells innervated through the corpus callosum in the cat. Exp Brain Res. 46:413–424.
Liu W, Suga N. 1997. Binaural and commissural organization of the primary auditory cortex of the mustached bat. J Comp Physiol A. 181:599–605.
Lomber SG. 1999. The advantages and limitations of permanent or reversible deactivation techniques in the assessment of neural function. J Neurosci Meth. 86:109–117.
Lomber SG, Cornwell P, Sun JS, MacNeil MA, Payne BR. 1994. Reversible inactivation of visual processing operations in middle suprasylvian cortex of the behaving cat. Proc Natl Acad Sci USA. 91:2999–3003.
Lomber SG, Malhotra S. 2008. Double dissociation of "what" and "where" processing in auditory cortex. Nat Neurosci. 11:609–616.
Lomber SG, Malhotra S, Hall AJ. 2007. Functional specialization in nonprimary auditory cortex of the cat: areal and laminar contributions to sound localization. Hear Res. 229:31–45.
Lomber SG, Payne BR. 2000. Translaminar differentiation of visually-guided behaviors revealed by restricted cerebral cooling deactivation. Cereb Cort. 10:1066–1077.
Lomber SG, Payne BR, Horel JA. 1999. The cryoloop: an adaptable reversible cooling deactivation method for behavioral or electrophysiological assessment of neural function. J Neurosci Methods. 86:179–194.
Marzi CA, Antonini A, Di Stefano M, Legg CR. 1982. The contribution of the corpus callosum to receptive fields in the lateral suprasylvian visual areas of the cat. Behav Brain Res. 4:155–176.
Merzenich MM, Knight PL, Roth GL. 1973. Cochleotopic organization of primary auditory cortex in the cat. Brain Res. 63:343–346.
Mitani A, Shimokouchi M. 1985. Neuronal connections in the primary auditory cortex: an electrophysiological study in the cat. J Comp Neurol. 235:417–429.
Morel A, Garraghty PE, Kaas JH. 1993. Tonotopic organization, architectonic fields, and connections of auditory cortex in macaque monkeys. J Comp Neurol. 335:437–459.
Nakamoto KT, Jones SJ, Palmer AR. 2008. Descending projections from auditory cortex modulate sensitivity in the midbrain to cues for spatial position. J Neurophysiol. 99:2347–2356.
Olfert ED, Cross BM, McWilliam AA. 1993. Guide to the care and use of experimental animals. Ottawa (ON): Canadian Council on Animal Care.

Palmer AR, Hall DA, Sumner C, Barrett DJ, Jones S, Nakamoto K, Moore DR. 2007. Some investigations into non-passive listening. Hear Res. 229:148–157.
Payne BR. 1990. Function of the corpus callosum in the representation of the visual field in cat visual cortex. Vis Neurosci. 5:205–211.
Payne BR, Pearson HE, Berman N. 1984. Role of corpus callosum in functional organization of cat striate cortex. J Neurophysiol. 52:570–594.
Payne BR, Siwek DF, Lomber SG. 1991. Complex transcallosal interactions in visual cortex. Vis Neurosci. 6:283–289.
Phillips DP, Irvine DR. 1982. Properties of single neurons in the anterior auditory field (AAF) of cat cerebral cortex. Brain Res. 248:237–244.
Pluto CP, Chiaia NL, Rhoades RW, Lane RD. 2005. Reducing contralateral SI activity reveals hindlimb receptive fields in the SI forelimb-stump representation of neonatally amputated rats. J Neurophysiol. 94:1727–1732.
Poremba A, Malloy M, Saunders RC, Carson RE, Herscovitch P, Mishkin M. 2004. Species-specific calls evoke asymmetric activity in the monkey's temporal poles. Nature. 427:448–451.
Reale RA, Imig TJ. 1980. Tonotopic organization in auditory cortex of the cat. J Comp Neurol. 192:265–291.
Reinoso-Suárez F. 1961. Topographischer Hirnatlas der Katz für experimentale physiologische Untersuchungen. [Topographical atlas of the cat brain for experimental-physiological research]. Darmstad, Federal Republic of Germany: Merck.
Rema V, Ebner FF. 2003. Lesions of mature barrel field cortex interfere with sensory processing and plasticity in connected areas of the contralateral hemisphere. J Neurosci. 23:10378–10387.
Rouiller EM, Simm GM, Villa AE, de Ribaupierre Y, de Ribaupierre F. 1991. Auditory corticocortical interconnections in the cat: evidence for parallel and hierarchical arrangement of the auditory cortical areas. Exp Brain Res. 86:483–505.
Ruttgers K, Aschoff A, Friauf E. 1990. Commissural connections between the auditory cortices of the rat. Brain Res. 509:71–79.
Schofield BR, Cant NB. 1996. Origins and targets of commissural connections between the cochlear nuclei in guinea pigs. J Comp Neurol. 375:128–146.
Tang J, Xiao Z, Suga N. 2007. Bilateral cortical interaction: modulation of delay-tuned neurons in the contralateral auditory cortex. J Neurosci. 27:8405–8413.
Thompson AM, Thompson GC. 1991. Projections from the posteroventral cochlear nucleus to the superior olivary complex in guinea pig: light and EM observations with the PHA-L method. J Comp Neurol. 311:495–508.
Weedman DL, Ryugo DK. 1996. Pyramidal cells in primary auditory cortex project to cochlear nucleus in rat. Brain Res. 706:97–102.
Winer JA. 1992. The Functional Architecture of the Medial Geniculate Body and Primary Auditory Cortex. In: Douglas W, Arthur P, Richard F, editors. The Mammalian Auditory Pathway: Neuroanatomy. New York: Springer-Verlag. p. 222–409.
Yang XF, Kennedy BR, Lomber SG, Schmidt RE, Rothman SM. 2006. Cooling produces minimal neuropathology in neocortex and hippocampus. Neurobiol Dis. 23:637–643.
Zurita P, Villa AE, de Ribaupierre Y, de Ribaupierre F, Rouiller EM. 1994. Changes of single unit activity in the cat's auditory thalamus and cortex associated to different anesthetic conditions. Neurosci Res. 19:303–316.